# Parametrization of Orthogonal Wavelet Transforms and Their Implementation

Peter Rieder , Jürgen Götze, Josef A. Nossek, and C. Sidney Burrus

*Abstract*— **In this paper a method for parameterizing orthogonal wavelet transforms is presented. The parameter space is given by the rotation angles of the orthogonal $2 \times 2$–rotations used in the lattice filters realizing the stages of the wavelet transform. Different properties of orthogonal wavelet transforms can be expressed in this parameter space. Then, the parameter space is restricted to the set of rotation angles given by simple orthogonal $\mu$–rotations, i.e. the set of rotation angles $\alpha_k = \arctan 2^{-k}$ ($k \in \{0, 1, \ldots w\}$ where $w$ is the wordlength). An orthogonal $\mu$–rotation is essentially one recursion step of the CORDIC algorithm. The wavelet transforms in the reduced parameter space are amenable to a very simple implementation. Only a small number of shift and add operations instead of fully fledged multipliers are required.**

## I. Introduction

In recent years different systems of wavelet bases have been introduced [3], [14] for a growing number of applications [1], [2], [4], [19]. Thereby the degrees of freedom existing in the design of wavelet bases have been exploited. Also methods have been presented to parameterize orthogonal wavelet transforms, whereby the optimization with respect to special properties is the primary intention of these parameterizations [6]. While most attention has been focussed on orthogonal, compactly supported wavelets with maximal number of vanishing moments, smoother, more regular wavelets were also designed [3]. Symmetry is an important property in image coding applications. Therefore, the design of least assymmetric, orthogonal wavelets is also an issue of the parameterization, although exact symmetry is impossible. In [6], [24] orthogonal wavelet transforms were optimized with respect to their frequency resolution after parameterizing the wavelet transforms of a certain compact support.

In this paper, a further property is added to the design constraints, namely the simple VLSI–implementation of the wavelet transforms. Orthogonal lattice filters [21] are often used to implement the stages of an orthogonal wavelet transform within a filterbank structure. These lattice filters can be implemented by orthogonal $2 \times 2$–rotations. The CORDIC algorithm [22], [23] offers one possibility to execute orthogonal rotations, whereby a sequence of $(w+1)$ $\mu$–rotations ($w$ being the wordlength) is used. These $\mu$–rotations can be implemented by a few shift- and add–operations. Let an orthogonal $\mu$–rotation be defined as one scaled (normalized) recursion step of the entire CORDIC sequence. We approximate the full sequence of $\mu$–rotations composing a rotation angle $\varphi$ by using only one or a few orthogonal $\mu$–rotations composing an approximate angle $\tilde{\varphi} \approx \varphi$. These approximate rotations were introduced in [9], [7] for efficiently computing the eigenvalue decomposition. This approach was not only extended to other iterative algorithms in signal processing [10], but also to orthogonal signal transforms [15], [13].

In order to parameterize all orthogonal wavelet transforms leading to a simple implementation, the following facts have been incorporated in the proposed approach:

1. Orthogonality is structurally imposed by using lattice filters consisting of orthogonal rotations only.
2. The sufficient condition for constructing a wavelet transform, namely one vanishing moment of the wavelet, is guaranteed, by assuring the sum of all rotation angles of the filters to be exactly $-45^o$ [24].
3. The full parameter space (i.e. arbitrary rotation angles) of all possible orthogonal wavelet transforms is restricted to a reduced parameter space that only allows rotation by the discrete angles $\alpha_k = \arctan 2^{-k}$ (basis angles of the CORDIC representation).
4. The constant sum of angles (see 2) is never violated by always using pairs of rotations with different signs independent of the rotation angles. Thereby, the rotations always appear twice, which also ensures a simple implementation of the scaling factor.

This paper is organized as follows: In Section II some preliminaries are given. In Section III the parameterization of orthogonal wavelet transforms is discussed and typical properties of wavelet bases are reviewed and expressed in the parameter space. Section IV defines orthogonal $\mu$–rotations that allow the efficient approximate implementation of elementary $2 \times 2$–rotations. In Section V the restriction of the full parameter space to the orthogonal $\mu$–rotation angles is outlined resulting in wavelet transforms which are simple to implement. Then, these wavelet transforms requiring only a few shift and add operations (per parameter) are compared to the standard wavelet transforms.

## II. Preliminaries

Using an orthogonal wavelet transform a continuous signal $s(t)$ is analyzed by translated versions $\Phi_{0,k}(t) = \Phi(t-k)$ of the scaling function $\Phi(t)$ at scale 0 and translated versions $\Psi_{j,k} = 2^{-j/2}\Psi(2^{-j}t - k)$ of the wavelet function $\Psi(t)$ at different scales $j$. For synthesis the same bases are used such that

$$s(t) \quad = \quad \sum_{k \in Z} \Phi_{0,k}(t) \int_{-\infty}^{+\infty} s(t) \Phi^*_{0,k}(t) dt$$

P. Rieder, J. Götze and J.A. Nossek are with the Inst. of Network Theory and Circuit Design, Technical University Munich, D-80290 Munich, Germany

C.S. Burrus is with the Dept. of Electrical and Computer Engineering MS-366, Rice University, Houston, TX 77251–1892, U.S.A.

$$+\sum_{j=0}^{\infty}\sum_{k\in Z}\Psi_{j,k}(t)\int_{-\infty}^{+\infty}s(t)\Psi_{j,k}^{*}(t)dt. \qquad (1)$$

In the frequency domain the wavelet series can be written as follows:

$$\begin{aligned}\hat{s}(\omega) &= \sum_{k}\hat{s}(\omega)\hat{\Phi}_{0,k}(\omega)\hat{\Phi}_{0,k}^{*}(\omega)\\ &\quad+\sum_{j}\sum_{k}\hat{s}(\omega)\hat{\Psi}_{j,k}(\omega)\hat{\Psi}_{j,k}^{*}(\omega), \qquad (2)\end{aligned}$$

where the Fourier transformation of a function $s(t)$ is defined as

$$\hat{s}(\omega)=\int_{-\infty}^{+\infty}s(t)\mathrm{e}^{-j\omega t}dt\,.$$

The functions $\Phi$ and $\Psi$ have to fulfill the dilation equations, that relate the continuous bases to the discrete coefficients $h_i$ and $g_i$:

$$\Phi(t)=\sum_{i=0}^{n-1}g_i\Phi(2t-i)\,,\qquad \Psi(t)=\sum_{i=0}^{n-1}h_i\Phi(2t-i)$$

With these coefficients $h_i, g_i \in \mathbb{R}$ the transfer functions of the discrete–time filters, which are used to implement the discrete wavelet transform can be formulated. These filters form one stage of the filterbank structure shown in Fig. 1, where the transfer functions are given by:

$$H(z)=\sum_{i=0}^{n-1}h_i z^{-i},\qquad G(z)=\sum_{i=0}^{n-1}g_i z^{-i}\,.$$

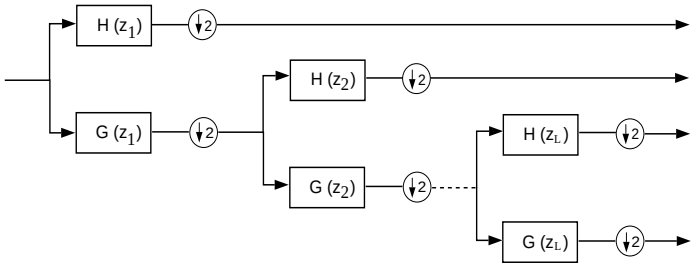


Fig. 1. Filterbank structure implementing a discrete wavelet transform

## III. Parameterization of Orthonormal Wavelet Transforms

An efficient structure for the implementation of orthogonal wavelet transforms (orthogonal, nonrecursive filters in general) is the lattice filter. The orthogonal filters of length $n$ $(H(z), G(z))$ can be implemented by a lattice filter using $n/2$ orthogonal rotations. The rotation angles $\beta_i$ $(i = 1,\ldots,n/2)$ are determined by the factorization either of $[G(z) \quad G(-z)]^T$ or $[G(z) \quad H(z)]^T$ into a shift product of orthogonal rotations [20], [5]. Theoretically (infinite wordlength) both factorizations yield the same result, but $[G(z) \quad H(z)]^T$ is numerically ill–conditioned as compared to $[G(z) \quad G(-z)]^T$. Fig. 2 shows a lattice filter implementation of one stage of Daubechies' wavelet transform of length $n = 4$. Obviously, the basic modules of the filter are orthogonal $2\times 2$ rotations. By using these orthogonal rotations orthogonality of the whole transform is structurally imposed [21] and therefore perfect reconstruction is simply possible.

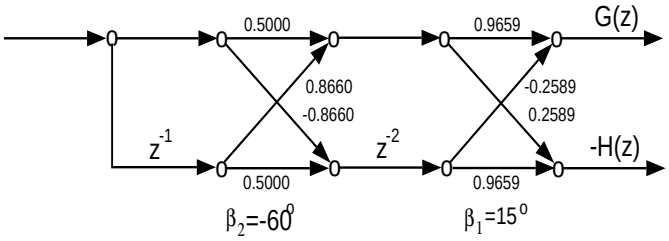


Fig. 2. Lattice filter implementing one stage of Daubechies' wavelet transform of length $n = 4$

In order to perform an orthogonal wavelet transform the lattice filter must fullfill another property. This property ensures that the wavelet function has zero mean which is equivalent to the wavelet having at least one vanishing moment and the transfer functions $H(z)$ and $G(z)$ having at least one zero at $z = 1$ and $z = -1$, respectively. These conditions are fullfilled if the sum of all rotation angles is exactly $-45^o$ [24], i.e.

$$\sum_{k}\beta_k=-45^o\,.$$

Therefore, a lattice filter whose sum of all rotation angles is $-45^o$ performs an orthogonal wavelet transform *independent* of the angles of each rotation.

A lattice filter of length $n$ consists of $n/2$ orthogonal rotations. Let $\beta_i$, $i = 1\ldots, n/2$ be the rotation angles of these $n/2$ orthogonal rotations. Then, by using the representation

$$\begin{aligned}\beta_1 &= -45^o-\varphi_1\\ \beta_i &= (-1)^i(\varphi_{i-1}+\varphi_i) \text{ for } i=2,\ldots,n/2-1 \qquad (3)\\ \beta_{n/2} &= (-1)^{n/2}\varphi_{n/2-1}\end{aligned}$$

all orthogonal wavelet transforms of length $n$ can be parameterized by the $n/2-1$ rotation angles $\varphi_i$. Note, that except for $i = 1$ and $i = n/2$ two rotations by the angles $\varphi_{i-1}$ and $\varphi_i$ are always required to implement the respective rotation angle $\beta_i$. Furthermore, note that each angle $\varphi_i$ appears twice in this representation.

In the following we will frequently use a wavelet transform of length $n = 6$ to illustrate the results. The parameterization consists of $n/2 = 3$ orthogonal rotations where the angles have the following representation

$$\begin{aligned}\beta_1 &= -45^o-\varphi_1\\ \beta_2 &= \varphi_1+\varphi_2 \qquad (4)\\ \beta_3 &= -\varphi_2.\end{aligned}$$

Of course, not all pairs of $(\varphi_1,\varphi_2)$ lead to a suitable wavelet transform. How the parameters $(\varphi_1,\varphi_2)$ are chosen depends

on the desired properties. These properties are discussed subsequently:

**Compact Support:** The compact support is equivalent to the finite length $n$ of the wavelet basis. While with $\varphi_1 \neq 0$ and $\varphi_2 \neq 0$, wavelets with support $n = 6$ can be constructed, by setting $\varphi_2 = 0$, the length is reduced to $n = 4$. If $\varphi_1 = \varphi_2 = 0$, one obtains the Haar basis ($n = 2$).

**Vanishing Moments:** The approximation properties of a wavelet basis are defined by the number of vanishing moments. In the continuous case, a wavelet with $p$ vanishing moments can represent a polynomial function up to degree $p - 1$ [3]. Therefore, wavelet systems are often designed in order to maximize the number of vanishing moments. This number $p$ is identical to the number of zeros of the transfer function $H(z)$ at $z = 1$. How many of the following equations are fullfilled by the coefficients $h_i$ determines the number of vanishing moments:

$$m_j = \sum_i i^j h_i = 0 \qquad j = 0, \ldots p-1. \tag{5}$$

In Fig. 3 (upper left) a Daubechies' wavelet of length $n = 6$ is shown. It has $p = 3$ vanishing moments, which requires the values of the parameters to be $\varphi_1 = 22.60^o$ and $\varphi_2 = 6.03^o$. Wavelet transforms with a maximal number of vanishing moments and length $n$ are called $O_n^D$ in this paper.

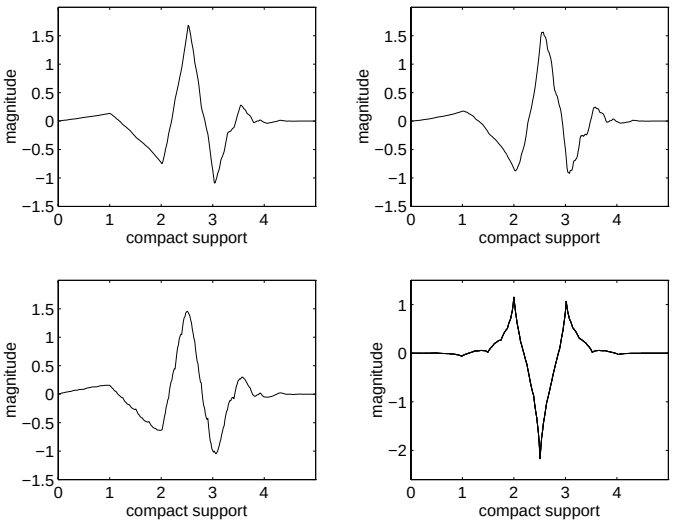


Fig. 3. Wavelet functions ($n = 6$) with certain properties: Version $O_6^D$ with maximal vanishing moments (upper left), most regular version $O_6^R$ (upper right), wavelet with best frequency behavior $O_6^F$ (lower left), and Coiflet $O_6^S$ (lower right)

**Regularity:** The fact, that wavelets with the maximal number of vanishing moments are not the only proper bases, was also in Daubechies' mind when she designed most regular, orthogonal wavelets [3]. Therefore, one task is to optimize the regularity of the orthogonal bases.

To precisely evaluate the regularity, the Hölder coefficient $r$ is widely used. A function, which is $d$ times continuously differentiable possesses a Hölder coefficient $r = d + e$, if its $d$th derivative $f^{(d)}$ is Hölder continuous with exponent $e$, i.e.

$$| f^{(d)}(x) - f^{(d)}(x+t) | \leq C \mid t \mid^e \forall x, t.$$

Some methods to compute the Hölder coefficient $r$ numerically were given in [16]. The analysis of the exact Hölder regularity usually causes high computational costs. In this paper a simple method to compute an upper bound of the Hölder coefficient $r$ is used, whereby the polynomial $G(z)$ is analyzed.

$$G(z) = (1 + z^{-1})^p F_p(z),$$

implies that the wavelet system has exactly $p$ vanishing moments. A matrix $\boldsymbol{F}_p$ defined by the coefficients of the polynomial $F_p(z)$ leads to an estimation of the Hölder coefficient. With $F_p(z) = f_{p,0} + f_{p,1} z + f_{p,2} z^2 + \ldots + f_{p,n-p} z^{n-p}$ the matrix $\boldsymbol{F}_p$ is given by

$$\boldsymbol{F}_p = \begin{bmatrix} f_{p,1} & f_{p,0} & 0 & \ldots & 0 \\ f_{p,3} & f_{p,2} & f_{p,1} & & \\ f_{p,5} & f_{p,4} & f_{p,3} & & \vdots \\ \vdots & & & \ddots & \\ 0 & & \ldots & & f_{p,n-p-1} \end{bmatrix}.$$

An upper bound $r$ for the Hölder coefficient is

$$r = p - 1 - \log_2 \max(| f_{p,0} |, | f_{p,n-p} |, \rho(\boldsymbol{F}_p)),$$

where $\rho(\boldsymbol{F}_p)$ is the spectral radius of $\boldsymbol{F}_p$. The spectral radius of $\boldsymbol{F}_p$ is defined as $\rho(\boldsymbol{F}_p) = \max_i(| \lambda_i |)$, where $\lambda_i$ denotes the eigenvalues of $\boldsymbol{F}_p$.

In contrast to Daubechies' wavelet ($n = 6$) with a maximal number of vanishing moments having a Hölder coefficient $r = 1.0878$, the most regular solution (called $O_n^R$) for $n = 6$ shows an increased smoothness as $r = 1.4176$ (Fig. 3, upper right). This solution requires $\varphi_1 = 26.06^o$ and $\varphi_2 = 8.40^o$.

It was shown in [3], if the wavelet function $\psi(t)$ of an orthogonal wavelet basis is $(p - 1)$ times continuously differentiable, then the wavelet function possesses $p$ vanishing moments. The converse, however, is not true since a wavelet function with $p$ vanishing moments only exhibits a degree of smoothness that asymptotically increases linearly by $\approx 0.2075 \cdot p$ [3]. Recently, this relationship (the gap) between the number of vanishing moments and the actual degree of smoothness has caused various approaches for the design of wavelet transformations, where the condition of possessing a maximal number of vanishing moments is waived. In [11] it was shown how one can systematically sacrifice higher order vanishing moments to achieve smoother wavelet (scaling) functions. Also, the meassure of smoothness for the design of wavelet basis in the discrete case (when continuous derivatives do not really exist) are discussed in [12] leading to a design of "smooth" wavelets in the discrete domain (i.e. regularity up to a certain scale $j$ of the discrete wavelet transform). The condition of vanishing moments will also be sacrificed in our approach for achieving a simple implementation of orthogonal discrete wavelet transforms.

**Frequency behavior:** As each stage of the wavelet transform is a pair of halfband filters, one optimization criterion is to place the roots of the coefficients of the scaling function such that an ideal lowpass is approximated as good as possible.

An orthogonal wavelet transform divides a signal into the different spaces spanned by the scaling function $\Phi_{0,k}$ and the wavelets $\Psi_{j,k}$. The reconstruction is based on the same bases as it is shown in (1). The wavelet series in the frequency domain is given in (2).

For the optimal solution the improvement of $\hat{\Phi}(\omega)$ with respect to its frequency behavior is not only necessary, but sufficient to improve the whole orthogonal wavelet system. Note that because of the orthogonality of spaces the wavelet $\hat{\Psi}$ is directly related to $\hat{\Phi}$. Therefore, improving the frequency behavior of $\hat{\Phi}(\omega)$ is equivalent to improving the frequency behavior of the whole transform.

The scaling function $\Phi$ can be determined from the dilation equation (given the discrete coefficients $h_i$). In the discrete case the discrete values of the scaling function are given by $\Phi(k)$. Using the vector representation $\mathbf{\Phi} = [\Phi(1), \ldots, \Phi(N)]^T$ the DFT yields $\hat{\mathbf{\Phi}} = [\hat{\Phi}(1), \ldots, \hat{\Phi}(N)]^T$:

$$\hat{\mathbf{\Phi}} = DFT(\mathbf{\Phi})\,. \tag{6}$$

The vector $\hat{\mathbf{\Phi}}$ can be divided into a passband part and a stopband part:

$$\hat{\mathbf{\Phi}} = \begin{bmatrix} \hat{\mathbf{\Phi}}_P \\ \hat{\mathbf{\Phi}}_S \end{bmatrix}, \tag{7}$$

where the upper $N/2^m$ elements of $\hat{\mathbf{\Phi}}$ belong to $\hat{\mathbf{\Phi}}_P$ and the remaining $N - N/2^m - 1$ elements of $\hat{\mathbf{\Phi}}$ belong to $\hat{\mathbf{\Phi}}_S$. While the elements of the passband part should contain large values, the elements of the stopband part should be small. Therefore, the norm $t = \|\hat{\mathbf{\Phi}}_S\|_2$ should be minimal. While the Daubechies wavelet with a maximal number of vanishing moments yields $t = 0.2119$, the best frequency behavior solution (called $O_n^F$) achieved for $n = 6$ with $\varphi_1 = 19.08^o$ and $\varphi_2 = 7.66^o$ leads to a stopband norm of $t = 0.1461$. In Fig. 4 the frequency characteristic of the respective scaling functions are compared and in Fig. 3 (lower left) the wavelet function with best frequency behavior is plotted.

**Symmetry:** Symmetry is a prefered property in some applications (e.g. image coding) but exact symmetry and orthogonality are not simultaneously possible. Therefore, least asymmetric wavelets were designed. In [3] Coiflets are discussed, which show an improved symmetry in comparison to standard wavelets. These Coiflets can be designed by requiring not only the wavelets to have vanishing moments but also the scaling functions. Additional to the equations (5) the discrete coefficients of these Coiflets fullfill the following equations:

$$\sum_i (n+1-i)^j h_i = 0 \qquad j = 0, \ldots p-1. \tag{8}$$

The parameters of a Coiflet transform (called $O_n^S$) for $n = 6$ and $p = 2$ are $\varphi_1 = -122.85^o$ and $\varphi_2 = -167.85^o$. The resulting wavelet function is plotted in Fig. 3 (lower right).

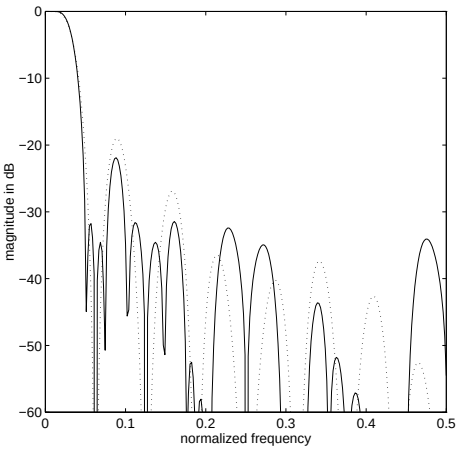


Fig. 4. Frequency characteristics of the standard wavelet transform ($O_6^D$, dotted line) and the version with best frequency behavior ($O_6^F$, solid line)

## IV. Efficient Implementation of Orthonormal Rotations

As shown in the previous section all orthogonal wavelet transforms can be implemented with a filterbank structure composed of lattice filters (see Figs. 1 and 2 as an example). The lattice filters consist of orthogonal $2\times2$–rotations $\boldsymbol{R}(\alpha)$ which are defined as follows:

$$\boldsymbol{R}(\alpha) = \begin{bmatrix} \cos\alpha & -\sin\alpha \\ \sin\alpha & \cos\alpha \end{bmatrix} = \tag{9}$$
$$= \frac{1}{\sqrt{1+\tan^2\alpha}} \begin{bmatrix} 1 & -\tan\alpha \\ \tan\alpha & 1 \end{bmatrix} (|\,\alpha\,| < 90^o).$$

The discretization $\tan\alpha_k = 2^{-k}$ leads to the rotation angles that are used by the CORDIC procedure [22], [23], which is a common method to execute orthogonal rotations with respect to a simple implementation. Any rotation is represented by a sequence of $(w+1)$ $\mu$–rotations ($w$ being the wordlength):

$$\boldsymbol{R}(\alpha) = \frac{1}{K_w} \prod_{k=0}^{w} \begin{bmatrix} 1 & -\sigma_k 2^{-k} \\ \sigma_k 2^{-k} & 1 \end{bmatrix}, \quad \sigma_k \in \{\pm 1\}, \tag{10}$$

with $\frac{1}{K_w}$ being the scaling factor that is independent of the angle $\alpha$

$$\frac{1}{K_w} = \prod_{k=0}^{w} \frac{1}{\sqrt{1+2^{-2k}}}\,. \tag{11}$$

This corresponds to the representation of the rotation angle $\alpha$ in the basis $\alpha_k = \arctan 2^{-k}$ with digits $\sigma_k \in \{\pm 1\}$:

$$\alpha = \sum_{k=0}^{w} \sigma_k \alpha_k = \sum_{k=0}^{w} \sigma_k \arctan 2^{-k}. \tag{12}$$

Now instead of using the entire sequence of basis angles $\alpha_k$ to represent $\alpha$ we restrict the set of available rotations to one specific recursion step of (10), i.e. the set of available

rotations is

$$\boldsymbol{R}(\alpha_k) = \frac{1}{\sqrt{1+2^{-2k}}} \begin{bmatrix} 1 & -\sigma_k 2^{-k} \\ \sigma_k 2^{-k} & 1 \end{bmatrix}, \sigma_k \in \{\pm 1\}, \tag{13}$$

$\boldsymbol{R}(\alpha_k)$ is called an orthogonal $\mu$–rotation and can be interpreted as an approximation of the rotation $\boldsymbol{R}(\alpha)$, if $\alpha_k$ is chosen such that it is the angle of the sequence $\alpha_k$ $(k = 0, 1, \ldots, w)$ which is closest to the exact rotation angle $\alpha$ [9], i.e.

$$\min_k |\alpha_k - \alpha| . \tag{14}$$

In [9] approximate rotations in form of orthogonal double $\mu$–rotations consisting of two equal orthogonal $\mu$–rotations (13) were used

$$\begin{aligned} \boldsymbol{R}(\bar{\alpha}_k) &= \boldsymbol{R}(\alpha_k)\boldsymbol{R}(\alpha_k) \\ &= \frac{1}{K_k^2} \begin{bmatrix} 1 & -\sigma 2^{-k} \\ \sigma 2^{-k} & 1 \end{bmatrix} \begin{bmatrix} 1 & -\sigma 2^{-k} \\ \sigma 2^{-k} & 1 \end{bmatrix} . \end{aligned} \tag{15}$$

The basis angles of the orthogonal double $\mu$–rotations are given by $\bar{\alpha}_k = 2\alpha_k$. The reason for using orthogonal double $\mu$–rotations is to avoid the square root of the scaling factor of an orthogonal $\mu$–rotation (13). The resulting scaling factor $\frac{1}{K_k^2}$ can be factored such that the scaling can be executed by shift and add operations. The factorization

$$\frac{1}{K_k^2} = \frac{1}{1+2^{-2k}} = (1-2^{-2k})(1+2^{-4k})(1+2^{-8k}) \ldots \tag{16}$$

leads to the following scaling procedure

$$\frac{1}{K_k^2} = (1-2^{-2k}) \prod_{s=1}^{b} (1+2^{-2^{s+1}k}) \quad \text{with} \quad b = \log_2 \lceil \frac{w}{2k} \rceil . \tag{17}$$

One orthogonal double $\mu$–rotation with a specific shift value $k$ chosen according to (14) is the basic element for approximating any orthogonal rotation of our parameterization of Section III. By using $r \ll w$ orthogonal double $\mu$–rotations an approximate rotation can be composed, that enables a simple implementation and approximates any orthogonal rotation to a certain accuracy.

## V. Restriction of the Parameter Space

For the parameterization of wavelet transforms, two items of Section III are important. The orthogonality of the transforms is structurally imposed by using lattice filters. By choosing the rotations such that the sum of angles is constant $-45^o$, the lattice structure always performs a wavelet transform. Therefore, the orthogonal $\mu$–rotation $\boldsymbol{R}(-45^o)$ always appears once in the presented wavelet filters:

$$\boldsymbol{R}(-45^o) = \boldsymbol{R}(-\alpha_0) = \frac{1}{\sqrt{2}} \begin{bmatrix} 1 & 1 \\ -1 & 1 \end{bmatrix} .$$

The scaling factor $1/\sqrt{2}$ does not need to be implemented. With each rotation appearing in the analysis part and in the synthesis part, also the scaling factor appears twice. As $1/\sqrt{2} \cdot 1/\sqrt{2} = 1/2$ can be implemented with one shift operation, the only price that must be paid is the loss of normality by a factor $1/\sqrt{2}$ in the transform domain.
By using only one (instead of $w+1$) $\mu$–rotation per parameter $\varphi_i$ of (3) the computational complexity is reduced significantly. We elaborate this in detail in our example (4). The two free parameters $\varphi_1$ and $\varphi_2$ of (4) are approximated by

$$\tilde{\varphi}_1 = \sigma_{\varphi_1} \arctan 2^{-k_{\varphi_1}} \qquad \tilde{\varphi}_2 = \sigma_{\varphi_2} \arctan 2^{-k_{\varphi_2}} .$$

The corresponding orthogonal $\mu$–rotations appear twice in our parameterization schemes (3). Therefore, it is always an orthogonal double $\mu$–rotation, which must be implemented (note the different sign in contrast to (16) since $\varphi_1$ and $\varphi_2$ each appear twice in (4) but with opposite signs). This implies that the simple realization of the scaling factor (16) can be applied.
The price one has to pay for the simplicity of the filters is, that the parameter space consisting of all possible rotation angles is reduced to a discrete parameter space spanned by the angles $\alpha_k = \arctan 2^{-k}$. But by using different parameterization schemes all having a constant sum of angles $\sum_k \beta_k = -45^o$, the grid of the reduced parameter space becomes more dense. Some of these schemes are given in Table I. The parameters $\varphi_1$ and $\varphi_2$ of the different schemes are not equal and one parameterization scheme might be better suited than the other for an approximation by the available set of $\mu$–rotation angles.

| S. | $\beta_1$ | $\beta_2$ | $\beta_3$ |
|---|---|---|---|
| 1 | $-45^o - \varphi_1$ | $\varphi_1 + \varphi_2$ | $-\varphi_2$ |
| 2 | $-45^o - \varphi_1 + \varphi_2$ | $\varphi_1$ | $-\varphi_2$ |
| 3 | $-90^o + \varphi_1$ | $45^o - \varphi_1 + \varphi_2$ | $-\varphi_2$ |
| 4 | $-90^o + \varphi_1 + \varphi_2$ | $45^o - \varphi_1$ | $-\varphi_2$ |
| 5 | $90^o - \varphi_1$ | $45^o + \varphi_2 + \varphi_1$ | $-180^o - \varphi_2$ |

TABLE I
Parameterization schemes for $n = 6$ wavelet transforms

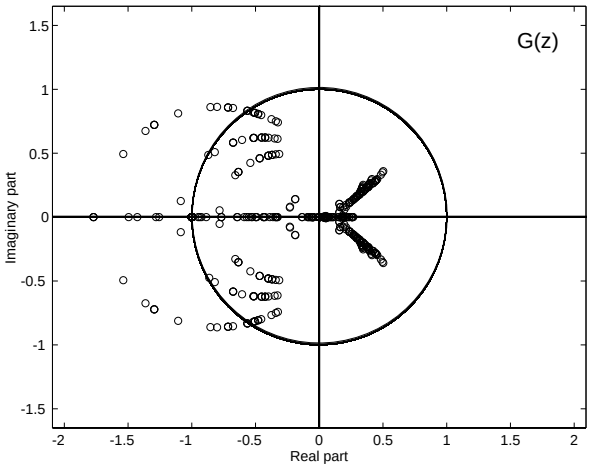


Fig. 5. Zero–distribution of $H(z)$ in the reduced parameter space

Fig. 5 shows the zeros of the polynomial $G(z)$ generated in the reduced parameter space with the parameteriza-

tion schemes 1–4 of Table I. Plotted are only those zeros, which are interesting with respect to the properties of compact support, vanishing moments, regularity and frequency behavior. The characteristic zeros are located close to $z = -1$, therefore, the area around this point is shown in detail. Though the parameter space is reduced to the domain of angles $\alpha_k = \arctan 2^{-k}$, the zero–distribution still allows the generation of wavelet transforms, whose zeros are placed close to $z = -1$ or close to the unit circle.

Besides the use of different parameterization schemes, another possibility for obtaining a denser grid is using other classes of orthogonal $\mu$–rotations [7]. Of course, one has always the possibility to increase the accuracy of the rotation approximation (equivalent to tighten the grid) by using more than one $\mu$–rotation per parameter.

The decisive question is whether or not the reduced parameter space leads to suitable alternatives to the optimal wavelets of Section III. Wavelet transforms were parameterized in the reduced parameter space that show the best performance with respect to the discussed properties (i.e. compact support, vanishing moments, regularity, frequency behavior and symmetry), whereby the parameters $k_{\varphi_1}$ and $k_{\varphi_2}$ of a certain parameterization scheme with the best performance are determined. In the Figs. 6–11 the plots of the scaling functions of the versions $\tilde{O}_4^D$, $\tilde{O}_4^R$, $\tilde{O}_6^D$, $\tilde{O}_6^R$, $\tilde{O}_6^F$, $\tilde{O}_6^S$ designed in the reduced parameter space (solid line) and the scaling functions belonging to the standard versions $O_4^D$, $O_4^R$, $O_6^D$, $O_6^R$, $O_6^F$, $O_6^S$ (dotted line) are compared. Also the zeros of $G(z)$ of the standard versions (upper right) and the approximate version (lower right) are given. The resulting lattice structure of the new versions showing the simple implementation (only very few shift and add operations are necessary) are given at the bottom of each Figure. Table II compares all solutions with respect to vanishing moments, regularity (upper bound), frequency behavior and rotation angles.

Obviously, the differences between the scaling functions showing the efficient implementation and the standard versions are very small. The comparison of the regularity $r$ and the stopband norm $t$ of the approximate and standard versions stresses the good performance of the wavelet transforms parameterized in the reduced parameter space. Of course, this is due to the small differences in the rotation angles, i.e. $\beta_k \approx \beta$. Only in the case of $\tilde{O}_6^R$ the smaller Hölder coefficient might be improved with an additional pair of $\mu$–rotations. Adding $\alpha_6$ to $\beta_2$ and subtract $\alpha_6$ from $\beta_3$ increases the upper bound of the regularity from $r = 1.0612$ to $r = 1.3714$, whereby the regularity of the standard solution ($r = 1.4176$) is almost achieved.

Since only one of the zeros of $G(z)$ is preserved exactly at $z = -1$ the number of vanishing moments is reduced to one by the approximation. Of course, this also affects the exact regularity of the continuous bases. For many applications, however, only the finite scale regularity of the (discrete) wavelet transform is essential, i.e. the regularity is evaluated only for a certain number of finite scales. This number is given by the actual number of stages used for the discrete wavelet transform. It is shown in [8] that the approxi-

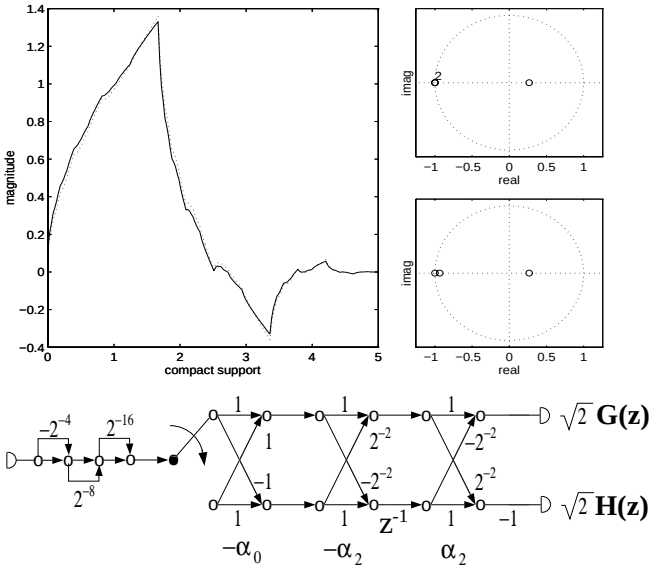


Fig. 6. Comparison of Daubechies' standard scaling function of length $n = 4$ ($O_4^D$, dotted line) and the version ($\tilde{O}_4^D$, solid line) showing the simple implementation

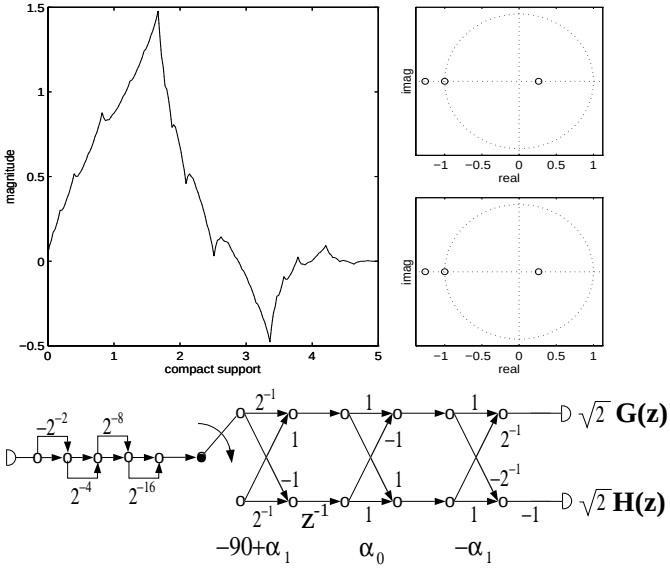


Fig. 7. More regular scaling functions of length $n = 4$ ($O_4^R$, dotted line, and $\tilde{O}_4^R$, solid line)

mate versions show a good finite scale regularity although the number of exactly vanishing moments is always $p = 1$ (higher moments only vanish approximately). In Fig. 12 the scaling function and the first and second numerical derivative of the original Daubechies scaling function $O_6^D$ ($p = 3$ vanishing moments; plots in the upper row) and the approximate scaling function ($m_0 = 0$, $m_1 = -0.0761$, $m_2 = -0.9247$; plots in the bottom row) are shown for the finite scale $j = 7$.

Obviously, the regularity of the scaling function is hardly degraded. This regularity can explicitly be analyzed using the discrete time definitions of regularity (slopes) in [17]. As long as the function and the respective *finite scale re-*

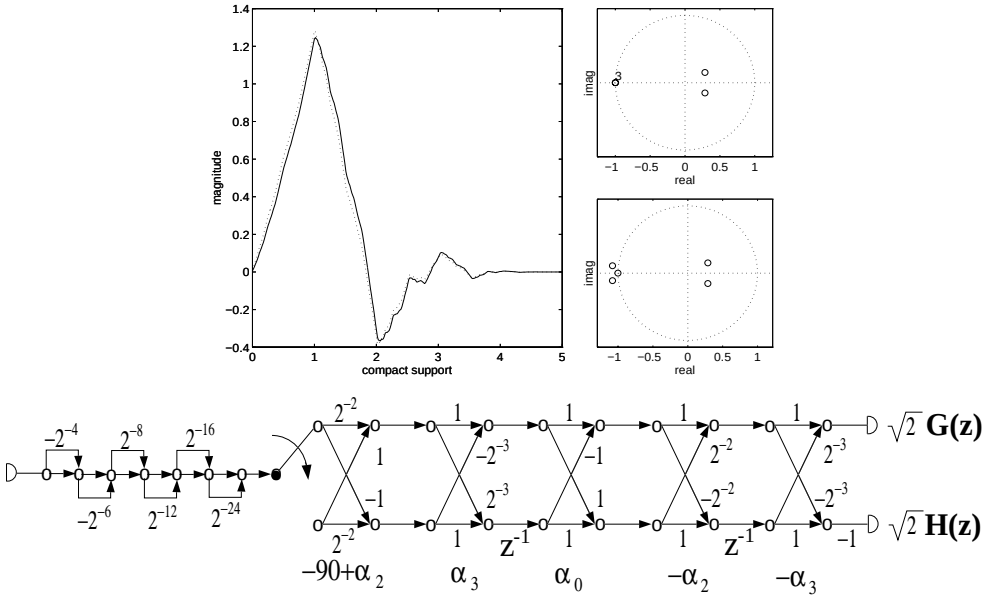


Fig. 8. Comparison of Daubechies' standard scaling function of length $n = 6$, ($O_6^D$, dotted line) and the version $\tilde{O}_6^D$, (solid line) showing a simple implementation

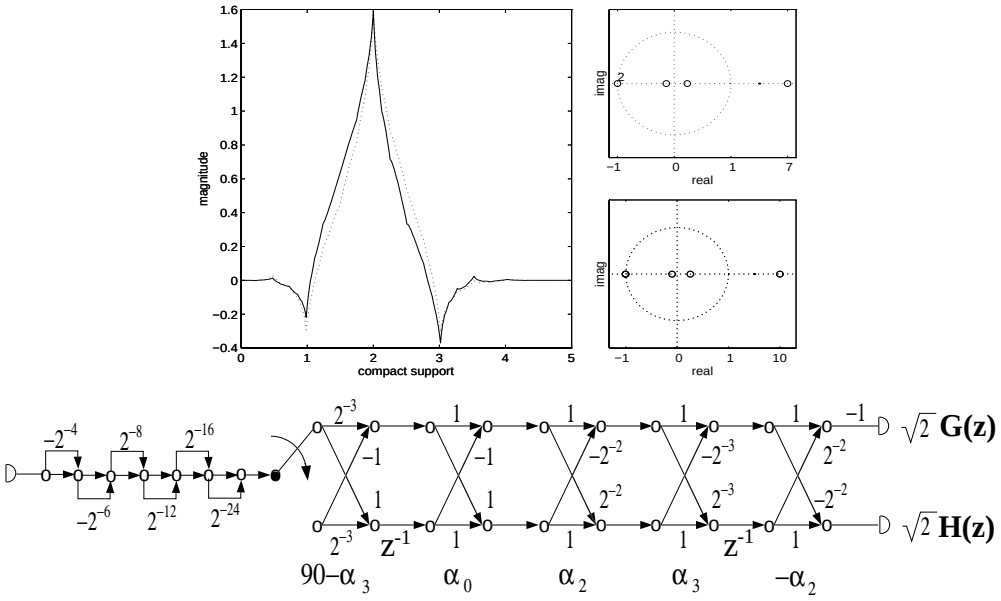


Fig. 9. More symmetric scaling functions of length $n = 6$ ($O_6^S$, dotted line, and $\tilde{O}_6^S$, solid line)

*gularity* show a reasonable behavior, the approximate discrete wavelet transform will be as well suited as the exact discrete wavelet transform. Note that the continuous approximate scaling function (i.e. for $j \to \infty$) is actually not differentiable. However, the finite scale regularity (slopes) is defined.

If the approach with one $\mu$–rotation does not guarantee the suitability of the discrete transform, of course, one has always the possibility of using more than one orthogonal $\mu$–rotation per parameter. Fig. 13 demonstrates the improvement of the approximation by using more than one $\mu$–rotation per parameter. The difference between the scaling function realized by the exact rotations and the scaling function realized by using $z$ $\mu$–rotations per parameter ($z = 1, 2, 3$) is shown for $O_6^D$.

## VI. Conclusion

In this paper a method was presented for parameterizing orthogonal wavelet transforms with respect to certain properties. Besides the standard properties (i.e. compact support, vanishing moments, regularity, frequency behavior, symmetry) a simple implementation of the wavelet transforms is also taken into consideration. Using only one simple orthogonal $\mu$–rotation per parameter (rotation angle of the lattice filter) guarantees the most simple implementation of the transform. Different parameterization schemes,

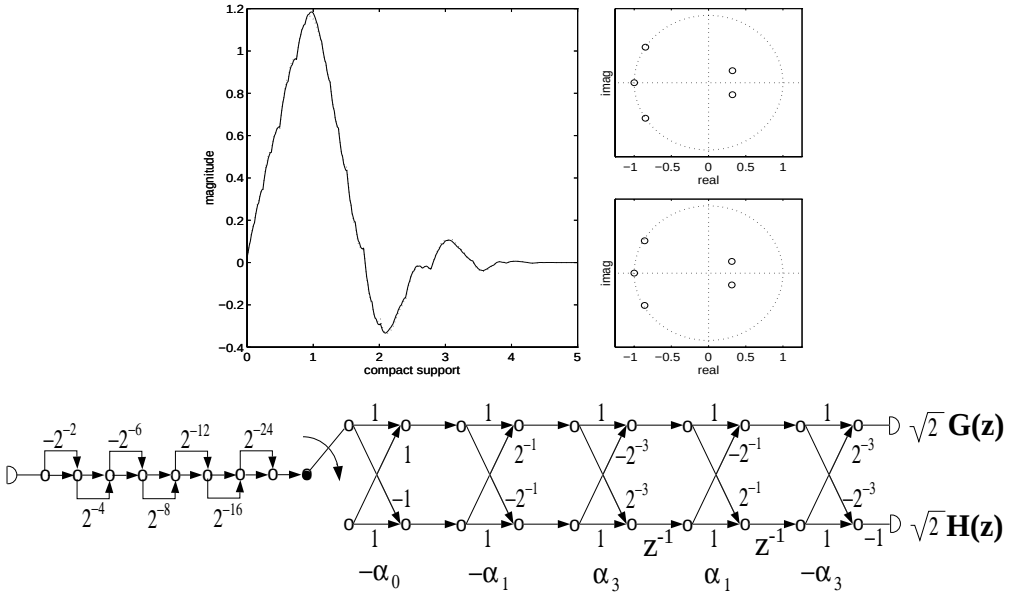


Fig. 10. Scaling functions with better frequency behavior ($O_6^F$ , dotted line, and $\tilde{O}_6^F$, solid line)

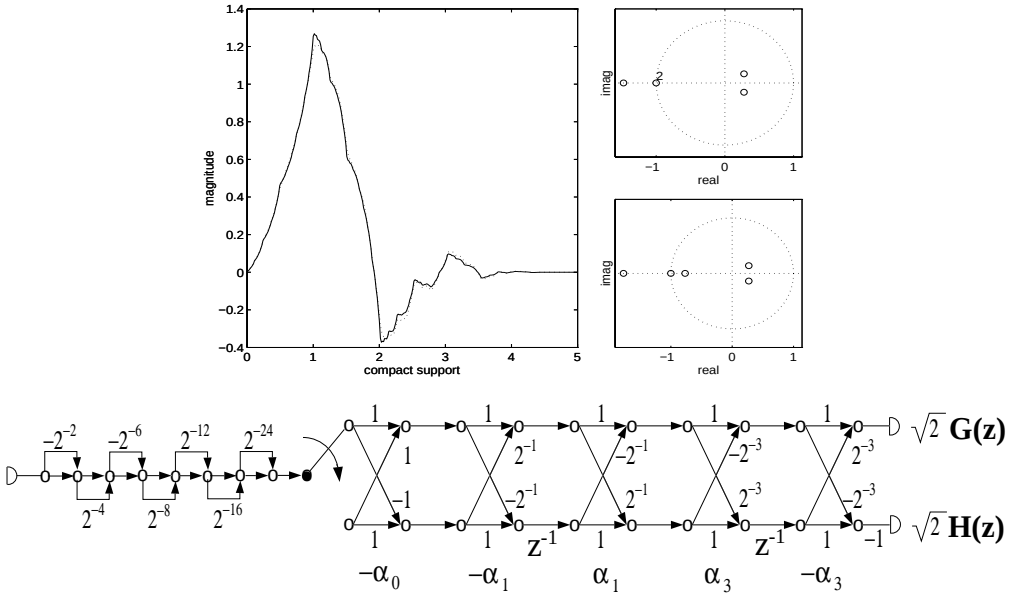


Fig. 11. More regular scaling functions of length $n = 6$ ($O_6^R$, dotted line, and $\tilde{O}_6^R$, solid line)

different types of $\mu$–rotations as well as more than only one $\mu$–rotation per parameter can be used to design wavelets which are closer to the standard versions. The most simple version (one $\mu$–rotation per parameter), however, already leads to wavelets which approximate the standard versions very well, such that for many practical applications these fast/simple wavelet transforms perform as good as the standard versions. Offering the possibility of a very simple implementation, the presented approach has already been used for an efficient VLSI–realization of discrete, orthogonal wavelet transforms [18].

## References


[1] B. Alpert, G. Beyklin, R. Coifman, and V. Rokhlin. Wavelet-like Bases for the Fast Solution of Second-Kind Integral Equations. *SIAM Journal on Sci. Comput.*, 14(1):159–184, January 93.

[2] M. Antonini, M. Barlaud, P. Mathieu, and I. Daubechies. Image Coding Using Wavelet Transform. *IEEE Transactions on Image Processing*, 1(2):205–220, April 92.

[3] I. Daubechies. *Ten Lectures on Wavelets.* Notes from the 1990 CBMS-NSF Conference on Wavelets and Applications at Lowell, MA. SIAM, Philadelphia, PA, 1992.

[4] D.L. Donoho. De–Noising by Soft–Thresholding. *IEEE Trans. Inform. Theory*, 41:613–627, 1995.

[5] G. Evangelista. Wavelet Transforms and Wave Digital Filters. In Y. Meyer, editor, *Wavelets and Applications*, pages 396–412. Springer–Verlag, 92.

[6] R.A. Gopinath, J.E. Odegard, and C.S. Burrus. Optimal Wavelet Representation of Signals and the Wavelet Sampling Theorem. *IEEE Trans. on Circuits and Systems II*, 41(4):262–277, April 1994.

[7] J. Götze and G.J. Hekstra. An Algorithm and Architecture ba-

| Version | $p$ | $r$ | $t$ | $\beta_1$ | $\beta_2$ | $\beta_3$ |
|---|---|---|---|---|---|---|
| $O_4^D$ | 2 | 0.5500 | 0.3517 | $-60.00^o$ | $15.00^o$ | 0 |
| $\tilde{O}_4^D$ | 1 | 0.5025 | 0.3533 | $-59.03^o$ | $14.03^o$ | 0 |
| $O_4^R$ | 1 | 0.7367 | 0.3706 | $-63.43^o$ | $18.43^o$ | 0 |
| $\tilde{O}_4^R$ | 1 | 0.7367 | 0.3706 | $-63.44^o$ | $18.44^o$ | 0 |
| $O_6^D$ | 3 | 1.0878 | 0.2119 | $-67.60^o$ | $28.63^o$ | $-6.03^o$ |
| $\tilde{O}_6^D$ | 1 | 1.0597 | 0.2109 | $-68.75^o$ | $30.97^o$ | $-7.12^o$ |
| $O_6^R$ | 2 | 1.4177 | 0.2315 | $-71.06^o$ | $34.46^o$ | $-8.40^o$ |
| $\tilde{O}_6^R$ | 1 | 1.0612 | 0.2109 | $-71.56^o$ | $33.68^o$ | $-7.12^o$ |
| $O_6^F$ | 1 | 0.8617 | 0.1461 | $-64.08^o$ | $26.74^o$ | $-7.66^o$ |
| $\tilde{O}_6^F$ | 1 | 0.8207 | 0.1480 | $-64.44^o$ | $26.56^o$ | $-7.12^o$ |
| $O_6^S$ | 2 | 0.5424 | 0.3399 | $77.85^o$ | $69.30^o$ | $-192.15^o$ |
| $\tilde{O}_6^S$ | 1 | 0.5341 | 0.3456 | $75.96^o$ | $66.16^o$ | $-187.12^o$ |

TABLE II

COMPARISON OF THE DIFFERENT VERSIONS OF ORTHOGONAL WAVELET TRANSFORMS

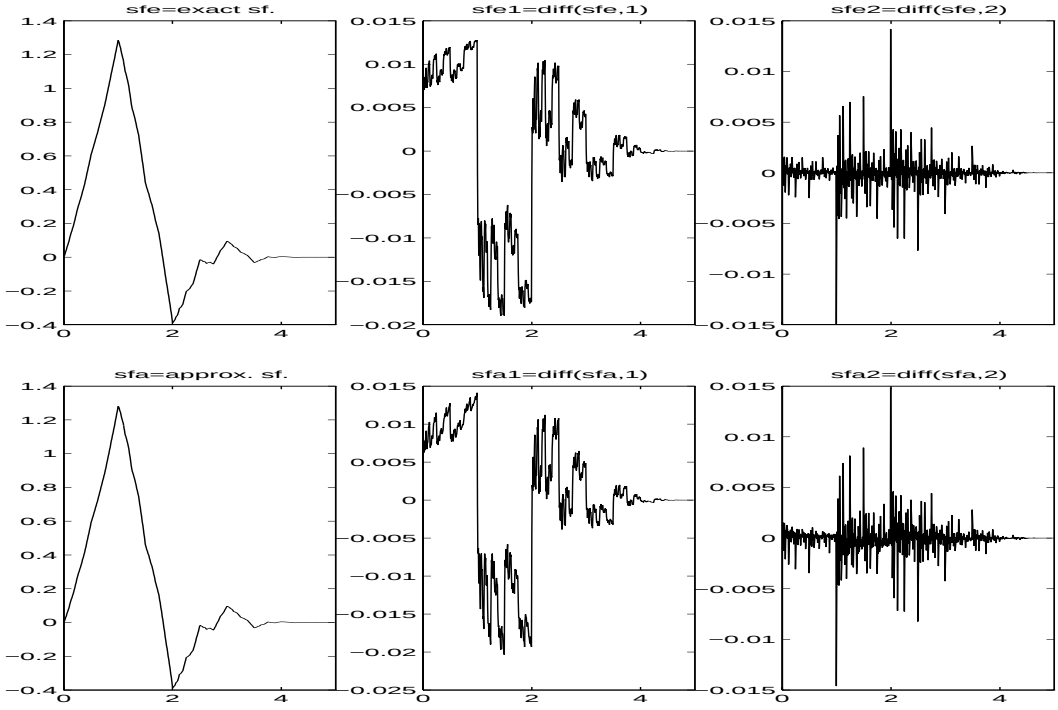


Fig. 12. Scaling function and 1st and 2nd discrete time derivative (slope) for Daubechies' filter $O_6^D$ (upper row) and for the approximate version $\tilde{O}_6^D$ (bottom row). Seven scales were used.

sed on Orthonormal $\mu$–Rotations for Computing the EVD. *INTEGRATION - The VLSI Journal. Special Issue on Parallel Algorithms and Architectures*, 20:21–39, 1995.

[8] J. Götze, J.E. Odegard, P. Rieder, and C.S. Burrus. Approximate Moments and Regularity of Efficiently Implemented Orthogonal Wavelet Transforms. *ISCAS, Atlanta*, II:405–408, Mai 1996.

[9] J. Götze, S. Paul, and M. Sauer. An Efficient Jacobi-like Algorithm for Parallel Eigenvalue Computation. *IEEE Trans. on Computers*, 42(9):1058–1065, September 1993.

[10] J. Götze, P. Rieder, and J.A. Nossek. Parallel SVD–Updating Using Approximate Rotations. *Proc. SPIE Advanced Algorithms and Architectures for Signal Processing*, pages 242–252, 1995.

[11] M. Lang and P.N. Heller. Design of Maximally Smooth Wavelets. *ICASSP, Atlanta*, III:1463–1466, Mai 1996.

[12] J.E. Odegard and C.S. Burrus. Towards a new Meassure of Smoothness for the Design of Wavelet Bases. *ICASSP, Atlanta*, III:1467–1470, Mai 1996.

[13] P. Rieder, K. Gerganoff, J. Götze, and J.A. Nossek. Parameterization and Implementation of Orthogonal Wavelet transforms. *ICASSP, Atlanta*, III:1515–1518, Mai 1996.

[14] P. Rieder, J. Götze, and J.A. Nossek. Algebraic Design of Discrete Multiwavelet Transforms. *Proc. IEEE Int. Conf. Acoust., Speech and Signal Processing, Adelaide*, III:17–20, April 1994.

[15] P. Rieder, J. Götze, M. Sauer, and J.A. Nossek. Orthogonal Approximation of the Discrete Cosine Transform. *In Proc. Europ. Conf. on Circuit Theory and Design ECCTD*, pages 1003–1006, August 1995.

[16] O. Rioul. Simple Regularity Criteria For Subdivision Schemes. *SIAM J. Math. Anal.*, 23(6):1544–1576, November 1992.

[17] O. Rioul. Regular Wavelets: A Discrete Time Approach. *IEEE Trans. on Signal Processing*, 41(12):3572–3579, December 1993.

[18] S. Simon, P. Rieder, C. Schimpfle, and J.A. Nossek. CORDIC-Based Architectures for the Efficient Implementation of Discrete Wavelet Transforms. *ISCAS, Atlanta*, IIII:77–80, Mai 1996.

[19] A.H. Tewfik and M. Kim. Fast Positive Definite Linear Sy-

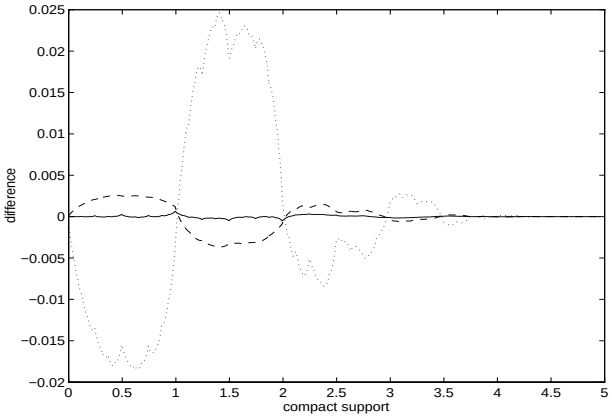


Fig. 13. Difference between the exact scaling function ($O_6^D$) and the approximate scaling functions using $z = 1$ (dotted line; $\tilde{O}_6^D$), $z = 2$ (dashed line) and $z = 3$ $\mu$–rotations per parameter of the exact realization.

stem Solvers. *IEEE Trans. on Signal Processing*, 42(3):572–585, March 1994.

[20] P.P. Vaidyanathan. *Multirate Systems and Filter Banks.* Prentice Hall, Englewood Cliffs, NJ, 1992.

[21] P.P. Vaidyanathan and P. Hoang. Lattice Structures for Optimal Design and Robust Implementation of Two-Channel Perfect-Reconstruction QMF Banks. *IEEE Trans. on ASSP*, 36(1), January 1988.

[22] J.E. Volder. The CORDIC trigonometric computing technique. *IRE Trans. Electron. Comput.*, EC-8:330–334, 59.

[23] J. Walther. A Unified Algorithm for Elementary Functions. *Joint Comput. Conf. Proc.*, 71.

[24] H. Xie and J.M. Morris. Design of Orthonormal Wavelets with Better Time-Frequency Resolution. *Proc. of SPIE, Wavelet Applications*, pages 878–887, 1994. Orlando,Florida.

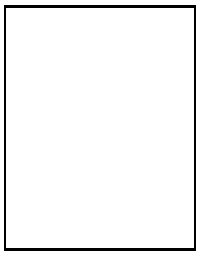

**Peter Rieder was Born in Germany on April 4, 1967. He recieved his Dipl.–Ing. degree in Electrical Engineering from the Technical University of Munich in 1993. Since 1993, he is with the Institute of Network Theory and Circuit Design at the Technical University of Munich, working on his Ph.D. degree.**
**His research interests include parallel algorithms, signal processing, especially multirate filterbanks and wavelets.**

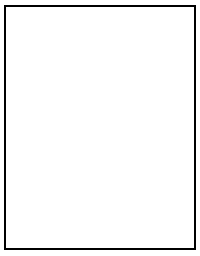

**Jürgen Götze received his Dipl.–Ing. and Dr.–Ing. degrees in Electrical Engineering from the Technical University of Munich in 1987 and 1990, respectively. From 1987 to 1990 he was with the Institute of Network Theory and Circuit Design, Technical University of Munich. From 1991 to 1992 he was with the Dept. of Computer Science, Yale University, sponsored by a research fellowship of the German National Science Foundation. From 1992 to 1995 he was with the Dept. of Electrical Engineering, Technical University of Munich. From 1995 to 1996 he was with the Department of Electrical and Computer Engineering, Rice University, sponsored by the Alexander von Humboldt foundation. Since 1996 he is again with the Technical University of Munich.**
**His research interests include numerical linear algebra, parallel algorithms, signal and array processing, wavelets.**

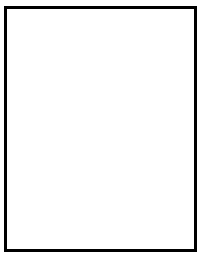

**Josef A. Nossek (S'72-M'74-SM'81-F'93), was born in Vienna, Austria, on December 17, 1947 and received the Diplom-Ingenieur and the Ph.D. degrees, both in electrical engineering, from the Technical University of Vienna, Austria, in 1974 and 1980, respectively. In 1974 he joined Siemens AG, Munich, Germany, where he was engaged in the design of passive and active filters for communication systems. In 1978 he became a supervisor, in 1980 head of a group of laboratories concerned with the design of monolithic filters (analog and digital) and electromechanical and microwave filters. In 1982 he became head of a group of laboratories designing digital radio systems within the Transmission Systems Department. In 1985 he spent a month as a visiting professor at the University of Capetown, South Africa. From 1987 to 1989 he was head of the Radio Systems Design Department. Since April 1989 he has been a full professor and head of the Institute of Network Theory and Circuit Design at the Technical University of Munich, Germany. He is teaching undergraduate and graduate courses in the field of circuit and system theory and conducting research in the areas of real-time signal processing, neural networks, and dedicated VLSI-architectures.**
**Dr. Nossek has published more than 100 papers in scientific and technical journals and conference proceedings. He holds a number of patents. In 1988 he received the ITG best paper award. From 1991 to 1993 he served as an associate editor of the IEEE Transactions on Circuits and Systems. Since 1995 he is Editor in Chief of the IEEE Transactions on Circuits and Systems, Part I: Fundamental Theory and Applications.**

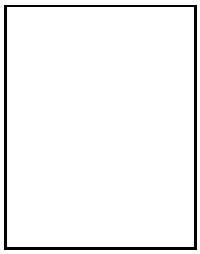

**C. Sidney Burrus was born in Abilene, TX, on October 9, 1934. He received the B.A., B.S.E.E., and M.S. degrees from Rice University, Houston, TX, in 1957, 1958 and 1960, respectively, and the Ph.D. degree from Stanford University, Stanford, CA, in 1965.**
**From 1960 to 1962, he taught at the Nuclear Power School in New London, CT, and during the summers of 1964 and 1965 he was Lecturer in Electrical Engineering at Stanford University. In 1965, he joined the faculty at Rice University where he is now Professor and Chairman of Electrical and Computer Engineering. From 1972 to 1978, he was Master of Lovett College at Rice University. In 1975 and again in 1979, he was a Visiting Professor at the Institut fuer Nachrichtentechnik, Universitaet Erlangen-Nuernberg, Germany, and in 1989–1990 he was a Visiting Professor at M.I.T.**
**Dr. Burrus is a member of Tau Beta Pi and Sigma Xi. He received teaching awards from Rice University in 1969, 1974, 1975, 1976, 1980, and 1989. He received an IEEE S–ASSP Senior Award in 1974, a Senior Alexander von Humboldt Award in 1975, a Senior Fulbright Fellowship in 1979, and the IEEE S–ASSP Technical Achievement Award in 1985. He was named an SP Society Distinguished Lecturer in 1991–1992 and was elected an IEEE Fellow in 1981. He is coauthor (with T.W. Parks) of two books: DFT/FFT and Convolution Algorithms and Digital Filter Design**